

Time resolved spectroscopic studies on some nanophosphors

HARISH CHANDER and SANTA CHAWLA*

Electronic Materials Division, National Physical Laboratory, Dr K S Krishnan Road,
New Delhi 110 012, India

Abstract. Time resolved spectroscopy is an important tool for studying photophysical processes in phosphors. Present work investigates the steady state and time resolved photoluminescence (PL) spectroscopic characteristics of ZnS, ZnO and (Zn, Mg)O nanophosphors both in powder as well as thin film form. Photoluminescence (PL) of ZnS nanophosphors typically exhibit a purple/blue emission peak termed as self activated (SA) luminescence and emission at different wavelengths arising due to dopant impurities e.g. green emission for ZnS: Cu, orange emission for ZnS: Mn and red emission for ZnS: Eu. The lifetimes obtained from decay curves range from ns to ms level and suggest the radiative recombination path involving donor–acceptor pair recombination or internal electronic transitions of the impurity atom. A series of ZnMgO nanophosphor thin films with varied Zn: Mg ratios were prepared by chemical bath deposition. Photoluminescence (PL) excitation and emission spectra exhibit variations with changing Mg ratio. Luminescence lifetime as short as 10^{-10} s was observed for ZnO and ZnMgO (100:10) nanophosphors. With increasing Mg ratio, PL decay shifts into microsecond range. ZnO and ZnMgO alloys up to 50% Mg were prepared as powder by solid state mixing and sintering at high temperature in reducing atmosphere. Time resolved decay of PL indicated lifetime in the microsecond time scale. The novelty of the work lies in clear experimental evidence of dopants (Cu, Mn, Eu and Mg) in the decay process and luminescence life times in II–VI semiconductor nanocrystals of ZnS and ZnO. For ZnS, blue self activated luminescence decays faster than Cu and Mn related emission. For undoped ZnO nanocrystals, PL decay is in the nanosecond range whereas with Mg doping the decay becomes much slower in the microsecond range.

Keywords. Photoluminescence (PL); time resolved decay; lifetime; nanophosphor.

1. Introduction

Time resolved spectroscopy is an important tool for studying energy and charge transfer processes, coupling of electronic and vibrational degrees of freedom, vibrational and conformational relaxation, isomerization, etc. The decay characteristics of phosphors could suggest the process of excitation and return to ground state and their time scale. It employs excitation by very short pulses of radiation like flash lamps, lasers etc, which can be spectrally tuned to the electronic transitions of the material to be studied. Doped nanophosphors have been the topic of intense research for their colour tunability and better luminescence efficiency leading to a wide variety of applications as light emitters in UV and visible (Bhargava *et al* 1994; Chander 2005). ZnS has been the workhorse as conventional phosphor whose application range included photoluminescence (PL), electroluminescence (EL) and cathodoluminescence (CL) devices. In the present study, ZnS nanophosphors have been doped with Cu, Mn and rare earth ion, Eu and the difference in photoluminescence and their decay characteristics due to dopant ion in

the same nanophosphor has been investigated. ZnO and its ternary alloy, ZnMgO, offer an excellent wide bandgap semiconducting material system with potential in applications related to quantum well and photonic devices in UV and visible. Earlier work on $Zn_xMg_{1-x}O$ thin film includes study of electrical and optical property (Kim *et al* 2006), bandgap variation with Mg content (Matsuhara *et al* 2003; Ogawa and Fujihara 2005), room temperature UV emission (Jin *et al* 2004). An understanding of the charge carrier dynamics in nanocrystalline semiconductor thin films is of much importance for their applications in PL and EL display devices.

Characterization of luminescence emission from a phosphor needs study of a few parameters like excitation and emission energy, luminescence efficiency, polarization and decay time. Excitation and emission spectra have been used routinely to identify luminescence characteristics of any phosphor. But time resolved spectroscopy of the luminescence decay provides an opportunity to probe into the temporal dynamics and the kinetics of the photophysical processes of the phosphor in the time domain. Towards this goal, the present study encompasses steady state PL and time resolved decay measurement of undoped and doped ZnS nanophosphors, ZnO and ZnMgO nanocrystalline thin films and powders.

*Author for correspondence (santa@mail.nplindia.ernet.in)

2. Experimental

2.1 Synthesis and film deposition

Undoped and Cu doped ZnS nanophosphor in thin film form was prepared by a wet chemical method using zinc acetate dihydrate, thiourea, urea, triethanolamine and copper (II) acetate monohydrate. ZnS:Eu nanophosphor was prepared by the same method by using europium nitrate solution instead of copper (II) acetate monohydrate. The reaction was carried out at 80°C under continuous stirring. ZnS:Mn was also prepared by wet chemical method (Karar *et al* 2004).

For wet chemical synthesis of ZnMgO with varied concentrations of Mg, precursor solutions of zinc acetate, magnesium chloride and triethanolamine were used. For deposition of film, precleaned glass slides were introduced vertically and chemical bath deposition was done at 80°C using a constant heating oil bath for times varying from 10 to 120 min. After the deposition, the glass slides were thoroughly cleaned with deionized water and dried in an oven at 50–80°C. Zn:Mg ratio was varied from 100:0 to 100:30 and good solubility was found in that range.

The typical solid state reaction method for synthesis of ZnMgO composites was as follows. Zinc oxide (1 M) was ground for 5 min and magnesium carbonate (0.2 M) was added to zinc oxide. After the mixture was ground for 20–30 min, the sample was packed in an alumina boat. Prior to use it was properly cleaned by HCl to make it free from impurities present in the boat. The packed sample was fired at ~1200°C for 3–5 h, using tube furnace with ammonia and nitrogen gas atmosphere.

2.2 Characterization

Structural characterization of the synthesized nanophosphors was done by XRD using Bruker-AXS D8 advance diffractometer with CuK α radiation. For nanophosphor thin films, glancing angle (1°) XRD profile was taken due to thinness of the deposited films. Morphology was studied with scanning electron microscope. Photoluminescence and time resolved decay of PL were measured in Perkin Elmer LS55 Fluorescence spectrometer and Edinburgh Instruments FLSP920 combined steady state Fluorescence and Phosphorescence lifetime spectrometer, respectively.

3. Results and discussion

3.1 Structure

XRD patterns of ZnS:Mn and ZnMgO nanophosphor are shown in figures 1(a) and (b), respectively. Particle size of the synthesized ZnS, estimated from XRD, SEM and TEM, was in the range 2–4 nm. XRD pattern of ZnMgO films

on glass substrate exhibit hexagonal wurtzite structure of ZnO (JCPDS card no 36-1451). The films show good crystalline structure (Chawla *et al* 2006). The particle size estimated from Scherrer formula was approximately 50 nm. The films hence essentially comprised of nano-

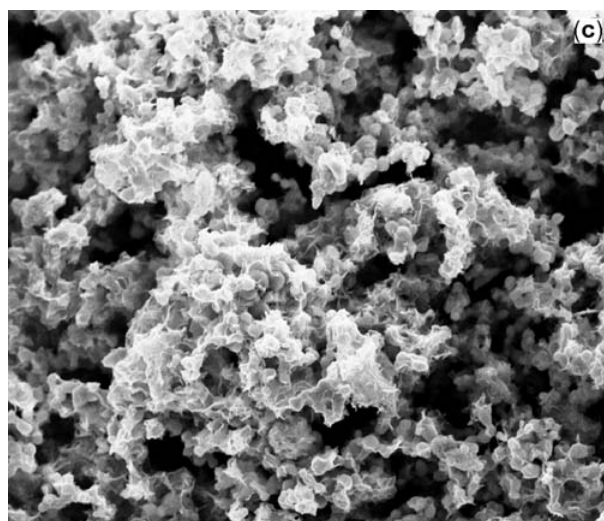
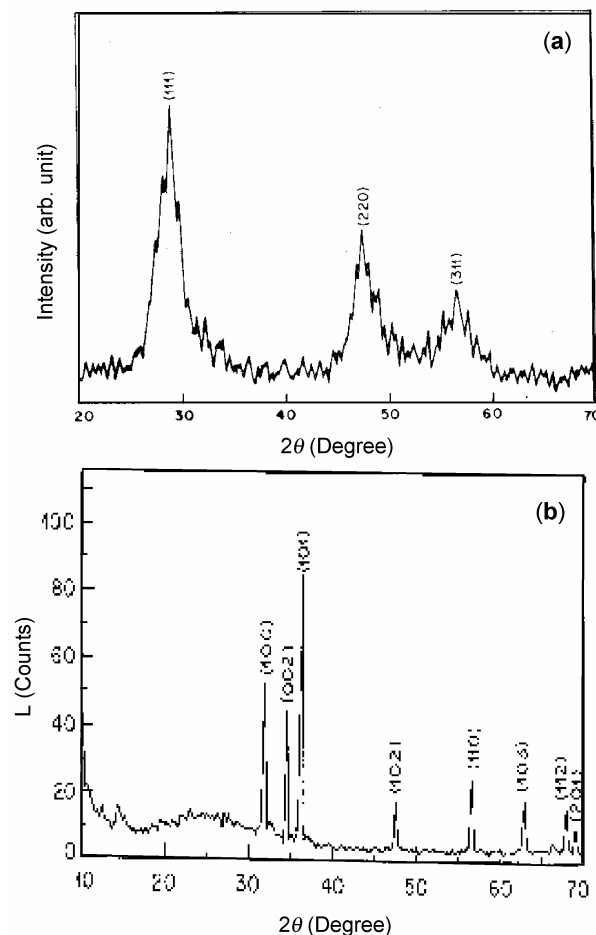


Figure 1. XRD pattern of (a) ZnS:Mn, (b) ZnMgO and (c) SEM micrograph of ZnMgO nanophosphor.

phosphor of ZnMgO with varied Mg ratio from 0 to 30% of Zn content. SEM micrograph of ZnMgO nanophosphor films indicates uniform distribution of particles. For the

samples prepared at $\sim 1200^\circ\text{C}$, ZnO and MgO phases were clearly identified by the presence of wurtzite ZnO and cubic diffraction peaks (Chander *et al* 2006). This fact indicated that the synthesized product was not a single phase but a composite. The average particle size of the ZnMgO powder sample was estimated to be ~ 35 nm. The SEM results (figure 1c) were consistent with XRD results. For ZnS nanophosphors, TEM was done and particle size estimated conform to XRD results.

3.2 Photoluminescence

PL excitation and emission spectra of undoped ZnS and ZnS : Cu, ZnS : Mn and ZnS : Eu are shown in figures 2(a), (b) and (c), respectively. Undoped ZnS nanophosphor showed two peaks at 390 nm and 430 nm. ZnS : Cu nanophosphors showed three PL emission peaks at 420, 480 and 525 nm. ZnS : Mn showed a prominent orange peak at 595 nm and a subdued 430 nm peak at 340 nm excitation. ZnS : Eu on the other hand exhibited a small peak at 430 nm

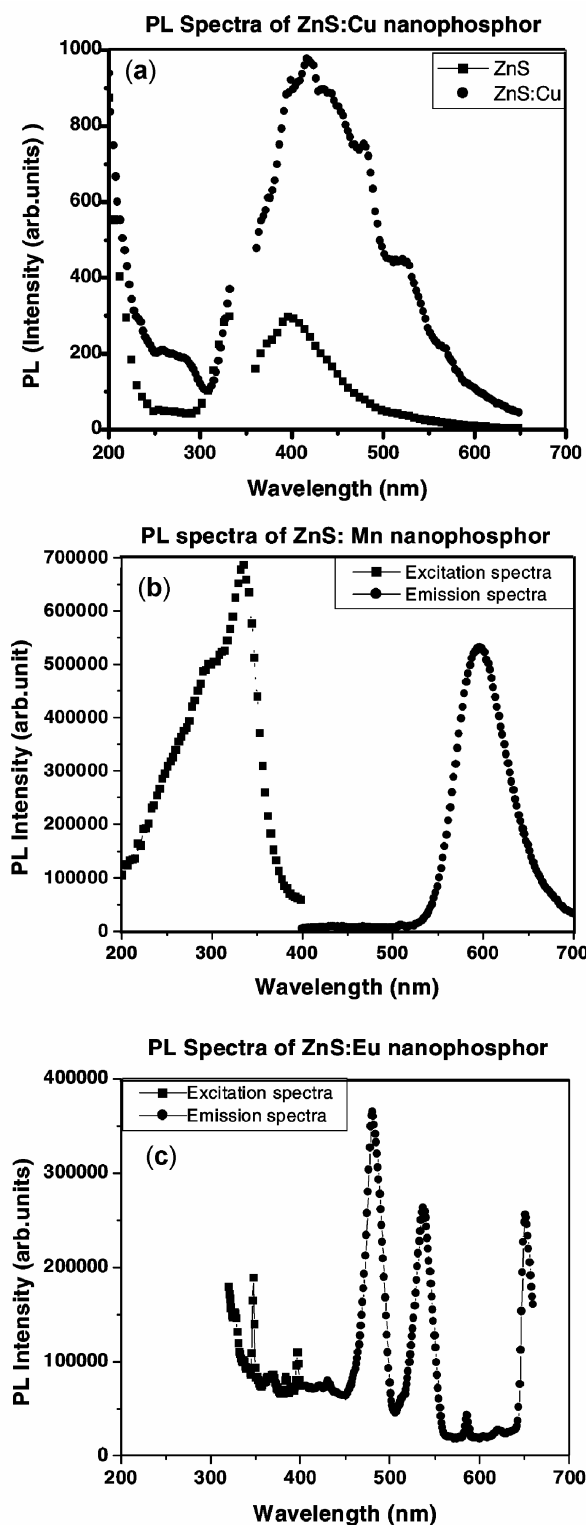


Figure 2. PL excitation and emission spectra of (a) undoped and Cu doped ZnS, (b) ZnS:Mn and (c) ZnS:Eu nanophosphor.

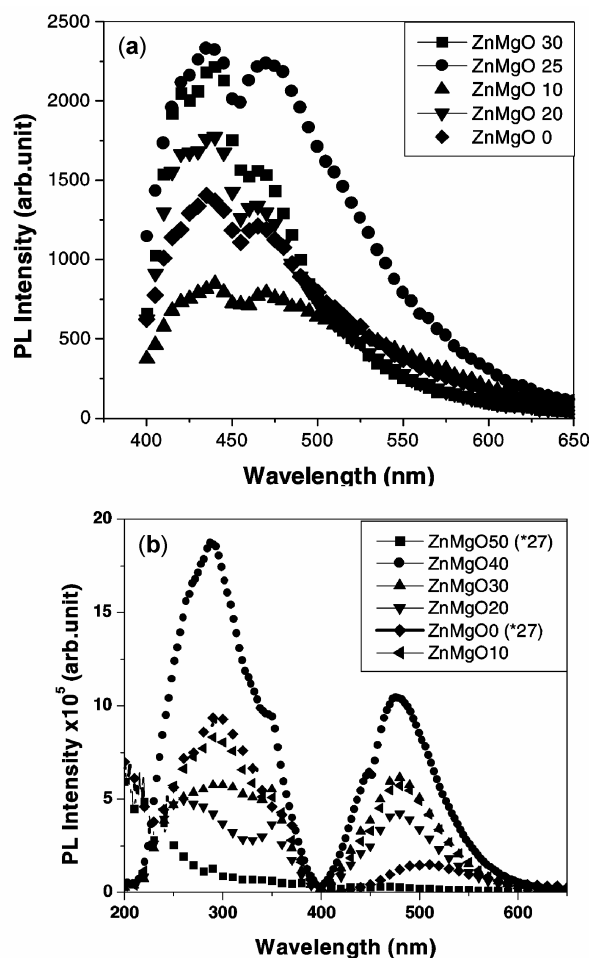
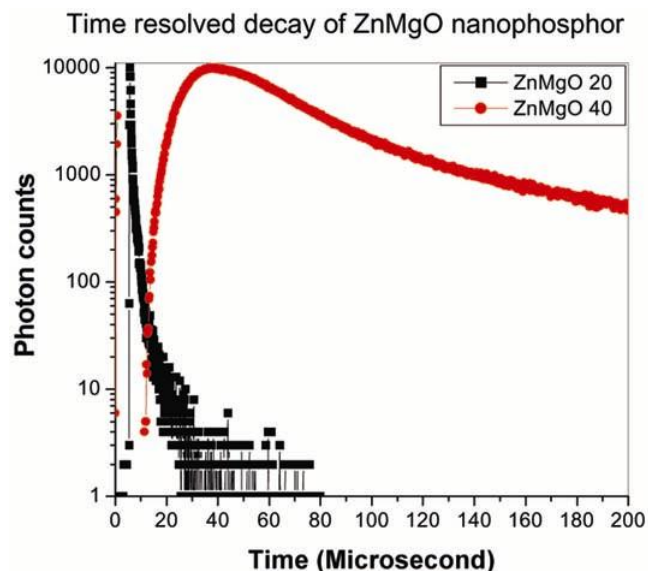


Figure 3. PL excitation and emission spectra of (a) ZnMgO nanophosphor thin films and (b) ZnMgO nanophosphor powder.

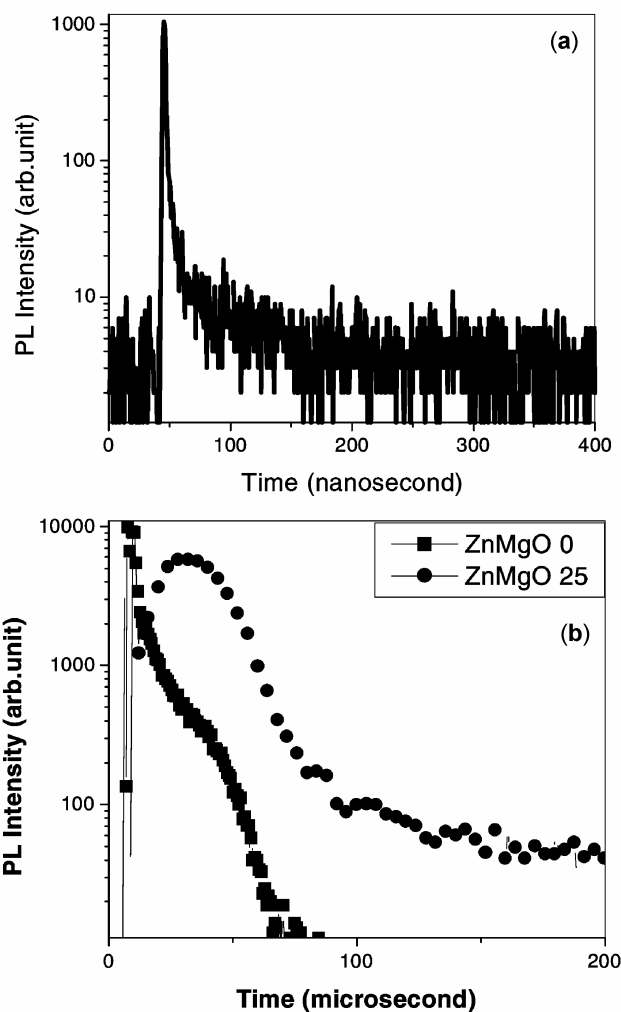
Table 1. Peak emission wavelengths of ZnS nanophosphors.

Phosphor	Peak 1 (nm)	Peak 2 (nm)	Peak 3 (nm)	Peak 4 (nm)
ZnS undoped	430			
ZnS : Cu	420	480	525	
ZnS : Mn	430	595		
ZnS : Eu	430	481	538	651

**Figure 4.** Time resolved luminescence decay of ZnMgO nanophosphor powders.

and sharp emission peaks characteristic of rare earth ions at 481, 538 and 651 nm. All the ZnS samples showed excitation peaks around 200 nm and 340 nm for 420–430 nm emission. However, the orange emission in ZnS : Mn was maximum with 340 nm excitation. Peak emission wavelengths for all ZnS phosphors are listed in table 1. The 420–430 nm peak in ZnS has been classically termed as self activated luminescence and known to be due to recombination of carriers between sulphur vacancy (V_S) related donor and valence bands (Lee *et al* 2004). The 480 nm blue peak has been observed in both ZnS : Cu and ZnS : Eu and hence may arise due to native point defect e.g. recombination from conduction band to a zinc vacancy. The 525 nm peak in ZnS : Cu is thought to be due to recombination between V_S and Cu related acceptor centre (Peng *et al* 2006).

Photoluminescence emission spectra of ZnMgO thin films under identical experimental parameters are shown in figure 3(a). The nanophosphor film with Zn : Mg composition ratio, 100 : 25, exhibit maximum PL output under same excitation conditions. The PL spectra appear to be superposition of a few peaks and could be deconvoluted into four peaks approximately situated at 420 nm, 440 nm, 462 nm and 500 nm.

**Figure 5.** Time resolved decay of ZnO nanophosphor thin film with (a) nanosecond flash lamp and (b) microsecond flash lamp.

The photoluminescence excitation and emission spectra of ZnMgO nanophosphor powders (figure 3b) showed that the intensity was maximum for ZnMgO with 40 mole% magnesium. The excitation spectra showed two prominent peaks, one around 290 nm and other around 350 nm whose position remained almost same for all the compositions. All the ZnMgO nanophosphor samples were then excited at 350 nm (3.5 eV). The emission spectra showed two peaks—one around 445 nm and a main peak at 508 nm in ZnO which blue shifts with increasing Mg content e.g.

Table 2. Decay parameters of PL peaks of ZnS : Cu nanophosphor.

Nanophosphor	Emission peak (nm)	τ_1 (μ s)	Relative (%)	τ_2 (μ s)	Relative (%)
ZnS undoped	420	0.69	61	5.12	39
ZnS : Cu 0.01 M	525	0.93	29	11.82	71
ZnS : Cu 0.1 M	525	0.89	19	9.82	81

Table 3. Decay parameters of PL peaks of ZnS : Mn nanophosphor.

Emission peak (nm)	τ_1 (μ s)	Relative (%)	τ_2 (μ s)	Relative (%)	Long decay component, τ (ms)	Long decay component relative (%)
430	2.14	7	14.65	93		
595	2.25	3	27.63	97	1.6	100

to 475 nm in ZnMgO (40 mole%) and 468 nm in ZnMgO (50 mole%).

3.3 Time resolved luminescence spectroscopy

Time resolved spectroscopy for luminescence lifetime measurement employed time correlated single photon counting technique. The sample was repetitively excited using a pulsed light source (ns flash lamp or μ s Xe flash lamp). Scanning over many pulses, the resultant decay curve viewed on a semilogarithmic scale, indicate the exponential/multiexponential or complex kinetics. Data analysis involves numerical deconvolution and a direct fit to the kinetic model. The decay curves could be expressed mathematically as

$$R(t) = A + \sum_{i=1}^n B_i e^{-t/\tau_i}, \quad (1)$$

where τ_i represents characteristic lifetime and denotes the time taken to decay from the beginning of the decay to 37% of the original value, B_i is a preexponential factor, which includes both instrumental and sample parameters. In a multiexponential decay, concentration ratio of individual components can be inferred from values of B_i . Two fitting routines are used, reconvolution fit and tail fit.

For extremely short exciting pulse, time resolved measurement showed a finite rising edge due to the exciting pulse. For precise estimation of short lifetimes the initial part of decay must be included in the analysis. Instrument response function plays an important role in the formation and initial decay part. In such case e.g. decay with nanosecond flash lamp (figure 5a), reconvolution fit routine has been employed after measuring the instrument response function *in situ*. Reconvolution fit routine allows one to fit over the rising edge of the data and eliminates both the noise and effects of the exciting pulse. Tail fit was applied for data which are fitted in a region with no further sample signal generation. Tail fit procedure

eliminates the statistical noise from the raw data but cannot handle the region of sample excitation. Tail fit has been used for analysis of longer decay time (figures 4, 5b, 6). In both the fit routines, iteration procedure was used for getting best set of decay parameters, B_i and τ_i . The 'goodness of fit' was ascertained by the reduced χ^2 value which has the theoretical limit, 1.

Time resolved decay of luminescence was recorded for ZnS : Cu, ZnS : Mn and ZnS : Eu nanophosphor at each peak emission wavelength (figure 6). The decay curves for ZnS : Mn (figure 6b) clearly indicate that while the 430 nm component almost completely decays in 70 μ s, the 595 nm component does so in 11 ms. Decay measurement of ZnS : Mn in 20 ms scale, gave a lifetime of the longer decaying component as 1.6 ms which matches well with reported value for cubic ZnS : Mn and the long lifetime was supposed to be due to the spin and parity forbidden transition (Bhargava *et al* 1994; Peng *et al* 2006). The μ s level decay times of 430 nm and 595 nm emissions may have the same origin in host ZnS lattice (Bol and Meijerink 1998). The results of luminescence lifetime measurements from fitting of single/multiexponential decay curves are listed in table 3.

It can be seen from table 2 that decay of undoped ZnS nanophosphor is faster than ZnS : Cu. Under larger than bandgap excitation (200 nm), the carrier dynamics involves band to band excitation, trapping at sulphur vacancy, recombination at valence band (420 nm emission) or Cu acceptor level (525 nm emission) and also conduction band to zinc vacancy acceptor centre (480 nm emission). As the decay time for DAP recombination is expected to be more and relative concentration of the longer decay component is more than 70% in ZnS : Cu, it may be inferred that faster decay component (0.69–0.93 μ s) is contributing to 420 nm emission and 11 μ s component is responsible for 525 nm emission. As the emission peaks are very closely spaced, more than one recombination is reflected in these decay times. Rare earth Eu dopant has been observed to decay in μ s time scale in different host crystals (Cho *et al* 2000) and our results also conform to

this. The 430 nm and 480 nm emissions are related to ZnS host lattice and showed biexponential decay. Whereas the

538 nm and 651 nm emission related to Eu ion give single decay time indicating isolation of the recombination process between Eu levels (table 4). Decay parameters of undoped ZnS bulk phosphor was measured and listed in table 5.

The decay curves for ZnMgO nanophosphor powders are shown in figure 4. The curve clearly shows that the decay becomes much slower for the nanophosphor samples with 40 mole% Mg ratio compared to 20 mole% Mg ratio. The decay curves could be fitted into exponential decay equations. The decay times for 20 mole% Mg ratio was 3 and 17 μs whereas 40 mole% Mg ratio nanophosphor showed a much longer decay time of 276 μs . The long decay times suggested that the luminescence may be produced due to donor-acceptor pair recombination.

For time resolved decay measurement of PL of ZnMgO nanocrystalline thin films (figure 5), the samples were excited at 350 nm with a nanosecond flash lamp and time resolved PL decay was recorded at 435 nm emission wavelength. Pure undoped ZnO and ZnMgO with 100 : 10 Zn : Mg ratio only exhibited decay in the nanosecond time scale. Other compositions do not show any decay in nanosecond timescale. Time resolved decay of ZnO and ZnMgO (100 : 25 Zn : Mg ratio) nanophosphor thin films measured with a Xe μs flash lamp is shown in figure 5b.

For time resolved decay measurements as shown in figure 5a, the life times were obtained from exponential reconvolution fit. Decay time obtained for ZnO was 0.56 ns (70%), 5.02 ns (14%) and 62.78 ns (16%). Similar decay times were also observed for ZnO nanocrystalline thin films of 20 nm particle size (Bauer *et al* 2004). From the measured life times it may be inferred that the recombination process is multiexponential.

All the nanophosphor thin films exhibit time resolved decay when excited with a μs pulse (figure 5b). Pure ZnO film showed fast decay with a lifetime of 6.47 μs . The other decay curve exhibited an initial growth and then decay, which could be fitted into a biexponential with lifetimes ranging from 5–8 μs and 20–70 μs with different contribution ratios with varying Mg content. Both the lifetime components, however, contribute equally in ZnMgO films with Zn : Mg ratio 100 : 25. Such long lifetimes are usually attributed to donor-acceptor pair (DAP) recombination. As the samples are zinc rich, Zn_i may act

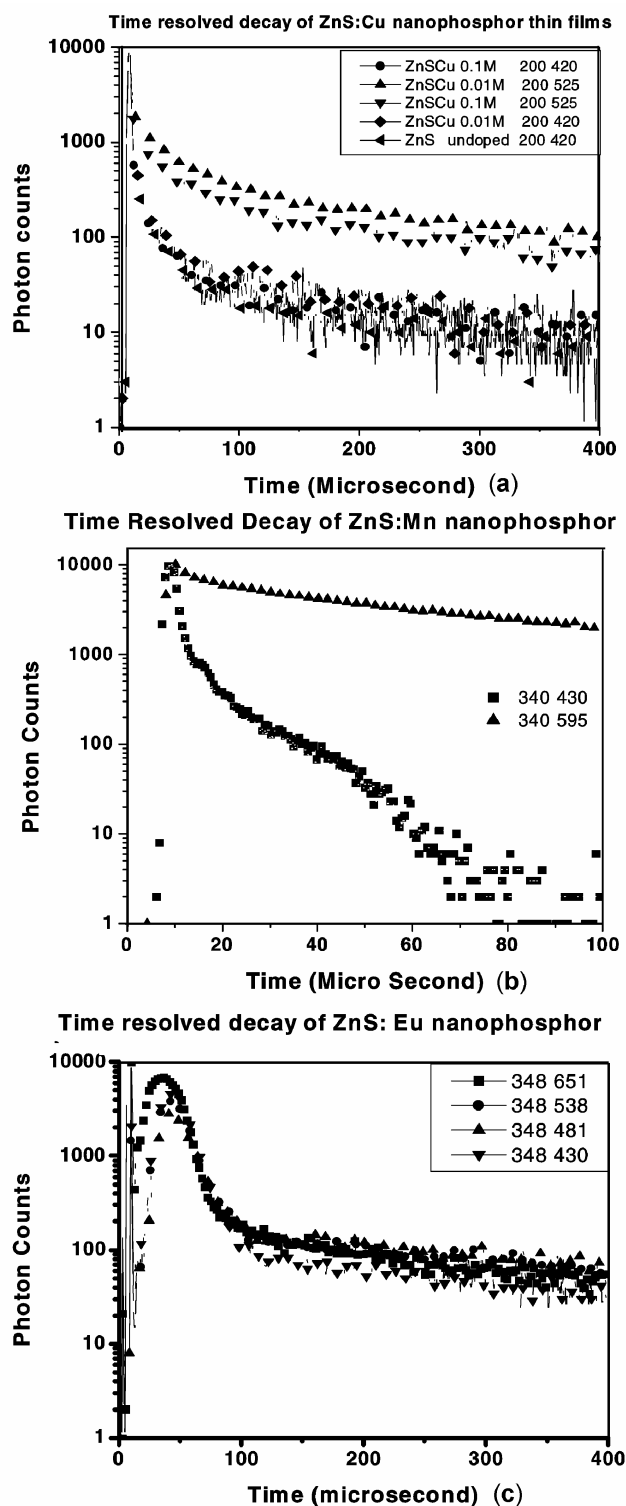


Figure 6. Time resolved decay of PL for (a) undoped ZnS and ZnS:Cu, (b) ZnS:Mn and (c) ZnS:Eu nanophosphors. The inset indicates the excitation and emission wavelengths at which time resolved decay measurements were done.

Table 4. Decay parameters of PL peaks of ZnS:Eu nanophosphor.

Emission peak (nm)	τ_1 (μs)	Relative (%)	τ_2 (μs)	Relative (%)
430	7.37	62	20.77	38
481	6.37	25	16.81	75
538	9.69	100		
651	8.99	100		

Table 5. Decay parameters of PL peak of undoped ZnS bulk phosphor.

Emission peak (nm)	τ_1 (μ s)	Relative (%)	τ_2 (μ s)	Relative (%)	τ_3 (μ s)	Relative (%)
430	2.49	18	6.18	44	17.75	38

as a shallow donor and radiative recombination may occur between donor level to deep acceptor levels.

4. Conclusions

ZnS nanophosphors doped with transition metal and lanthanide atoms were prepared successfully by wet chemical method. ZnS nanophosphors could be tuned to emit any colour from purple/blue to green (ZnS:Cu), orange (ZnS:Mn) and red (ZnS:Eu) by choosing the proper dopant. Time resolved decay showed faster decay times for purple/blue emission (SA) and microsecond level decay time for impurity emission and shed light on possible carrier dynamics of the recombination process.

Study of steady state PL of ZnMgO nanophosphor thin films with varying Mg ratio show that the luminescence in the visible region (blue) enhances significantly with changing Zn:Mg ratio, reaching a maximum for 100:25 ratio. Time resolved decay measurement shows carrier dynamics with charge trapping in a time scale of hundreds of picosecond. All of the nanophosphor thin films also show luminescence arising from DAP recombination happening in microsecond timescale.

The study of optical properties of ZnMgO nanocomposites in the nanocrystalline form shows very clearly that it is possible to obtain enhanced luminescence properties in the visible region by changing the ratio of Mg content. The enhancement of luminescence of ZnMgO (40 mole% Mg) is about 62 times compared to pure ZnO prepared by

the same synthesis method. The enhancement of luminescence is also associated with a slow decay component, which could be due to deep traps created in the high Mg ratio nanocomposites. Such nanocomposites hence could be very good nanophosphors for various display purposes.

References

- Bauer C, Boschloo G, Mukhtar E and Hagfeldt A 2004 *Chem. Phys. Lett.* **387** 176
- Bhargava R N, Gallagher D, Hong X and Nurmikko A 1994 *Phys. Rev. Lett.* **72** 416
- Bol A A and Meijerink A 1998 *Phys. Rev.* **B58** R15 997
- Chander H 2005 *Mater. Sci. & Eng.* **R49** 113
- Chander Harish, Chawla Santa, Jayanthi K and Kar M 2006 *Proc. Indo-Japan workshop on ZnO materials and devices* (ed.) R M Mehra *et al* (Pentagon Press) pp 9–11
- Chawla Santa, Jayanthi K and Chander Harish 2006 *Proc. Indo-Japan workshop on ZnO materials and devices* (ed.) R M Mehra *et al* (Pentagon Press) pp 12–14
- Cho A *et al* 2000 *J. Lumin.* **91** 215
- Jin Y *et al* 2001 *Solid State Commun.* **119** 409
- Karar N, Singh F and Mehta B R 2004 *J. Appl. Phys.* **95** 656
- Kim J W, Kang H S, Kim J H and Lee S Y 2006 *J. Appl. Phys.* **100** 033701
- Lee S *et al* 2004 *Mater. Lett.* **58** 342
- Matsuhara K *et al* 2003 *Mater. Res. Soc. Symp. Proc.* **763** B7.2.1
- Ogawa Y and Fujihara S 2005 *Phys. Status Solidi (a)* **202** 1825
- Peng W Q, Cong G W, Qu S C and Wang Z G 2006 *Opt. Mater.* **29** 313